Fishbones Activity in JET Low Density Plasmas

F. Nabais 1), D. Borba 1), M. Mantsinen 2), S. Sharapov 3) and JET-EFDA contributors[1]

1) Association EURATOM/IST, Av. Rovisco Pais, 1049-001 Lisboa, Portugal
2) Association EURATOM/TEKES, Helsinki University of Technology, Espoo, Finland
3) EURATOM/UKAEA Fusion Association, Culham Science Centre, Abingdon, OX14 3DB, U.K.

e-mail contact of the main author: fnabais@cfn.ist.utl.pt

Abstract. Fishbone activity with frequencies around the precessional drift frequency of the fast ions and the diamagnetic frequency of the bulk ions have been observed in several tokamaks. In the first case, fishbone bursts occur when the precessional fishbone branch of the internal kink mode becomes unstable, while in the second case fishbone bursts are caused by the ion branch, which corresponds to a different solution of the same dispersion relation. JET discharges carried out with low density plasmas and high ICRH power provided a scenario where the precessional fishbone branch and the ion branch coalesced. In this case, two new fishbones regimes were observed: a regime where fishbone bursts covered both ranges of frequencies showing hybrid characteristics, and a regime where low amplitude bursts of both types of fishbones occurred simultaneously. These coalescent regimes may also be reached if the radius of the q=1 surface is large, as it is predicted to be in ITER. Fishbone activity is analysed by means of a variational formalism that allows the calculation of the regions of stability for each branch in the space of parameters upon which the fishbone stability depends. This allows not only the analysis of experimental results but also the prediction of how fishbone stability would evolve in different circumstances, depending on the evolution of the relevant parameters.

1. Introduction

Fishbone activity [1] with frequencies around the precessional drift frequency of the fast ions $\omega \sim \omega_{DH}$ [2] are commonly observed in many tokamaks when the fast ions beta β_h (kinetic pressure / magnetic pressure) is sufficiently high. These fishbones, which in this paper will be referred to as precessional fishbones, are caused by the fishbone branch of the internal kink mode. The fishbone branch is not a "normal solution" of the MHD dispersion relation, it only appears as solution of the dispersion relation when the fast ions energy functional δW_{HOT} is included. Thus, its existence is dependent on the presence in the plasma of a fast ions population. The growth rate of this mode goes to $-\infty$ ($\gamma \rightarrow -\infty$) as $\beta_h \rightarrow 0$, but it increases when increasing β_h and the mode becomes unstable for values of β_h above a critical value, causing precessional fishbone bursts to occur. Fishbone bursts can also be observed at low values of β_h, but in this case, fishbones appear at frequencies around the diamagnetic frequencies of the bulk ions $\omega \sim \omega_{*i}$ [3]. Fishbones of this type, which in this paper will be referred to as diamagnetic fishbones, are caused by the ion branch of the internal kink mode. The ion branch appears as solution of the dispersion relation when diamagnetic effects are introduced and it can become unstable if the diamagnetic frequency sufficiently high. However, to turn the mode unstable it is also needed the presence in the plasma of fast ions to tap the source of energy for the instability, which is related to the pressure gradient of the plasma bulk. Thus, two different types of fishbone bursts have been usually observed, being caused by two different branches of the internal kink mode: the fishbone branch, which is associated with fast ion effects and that becomes unstable when the critical parameter β_h is sufficiently high, and the ion branch, which is associated with diamagnetic effects and that requires ω_{*i} to be sufficiently high for instability to be possible. Usually, the precessional fishbones regime is observed for high values of β_h while the diamagnetic fishbones regime is observed for low

[1] See appendix of J. Pamela et al., "Overview of JET Results" OV/1-2, Fusion Energy 2004, IAEA, (2004)

values of β_h, being both regimes separated by a stable window. When the diamagnetic frequency of bulk ions is significantly lower than the precessional drift frequency of the fast ions, $\omega_{*i} << \omega_{DH}$, it is also possible classify the fishbones regimes as high frequency fishbones and low frequency fishbones. Aside from the fishbone branch and the ion branch, the internal kink mode dispersion relation has the "normal MHD" solution, the kink branch. The kink branch becomes unstable when the ideal growth rate γ_I is sufficiently high, causing sawteeth to occur (γ_I is defined as $\gamma_I \equiv -\omega_A \delta W_{MHD}$, where ω_A is the Alfven frequency and δW_{MHD} is the usual minimized variational energy for the internal kink mode [4]).

In JET experiments with low density plasmas and where the only auxiliary heating used was ICRH (Ion Cyclotron Resonance Heating), aside from high and low frequency fishbones, two new fishbones regimes were observed: a regime of fishbones covering both high and low frequencies and a regime where high and low frequency fishbones occur simultaneously. These experimental results are presented in Sec. II. In Sec. III, the regions of stability for each branch of the internal kink mode in the space of parameters ($\beta_h, \omega_{*i}, \gamma_I$) are presented. In Sec. IV the changes in the regions of stability and the evolution of the parameters (β_h, ω_{*i}, γ_I) are determined, allowing a theoretical explanation for the appearance of the two new fishbone regimes. In Sec. V the dependence on frequency of the resonant exchange of energy and the types of orbits of the resonant particles are shown. Finally, in Sec. VI, conclusions are drawn.

2. New experimental results

Recent JET experiments carried out with low density plasmas and high power of ICRH provided a scenario where fishbone behaviour was observed to change during the period of a monster sawtooth. Sawtooth stability was also observed to change during the discharges, being related to the plasma density. In fact, there was a threshold in density above which sawtooth was stable and below which was unstable [5]. When unstable, sawteeth were observed along with precessional fishbones. After sawteeth being stabilized (following an increase in the plasma density), fishbones behaviour was observed to change gradually from high frequency fishbones to low frequency fishbones. In intermediate stages, two new fishbones regimes were observed: a regime of fishbones covering both ranges of frequencies and a regime where both types of fishbones occur simultaneously (see fig.1).

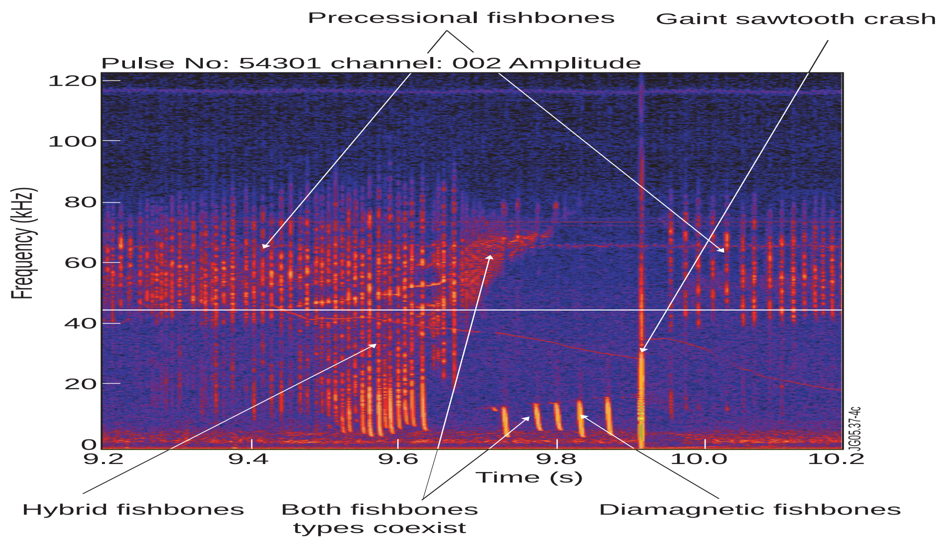

Figure 1: Spectrogram showing the evolution of fishbones behaviour along a monster sawteeth.

After a sawtooth crash it is always observed the regime of precessional fishbones. This regime evolves to a regime of fishbones covering both high and low frequencies (around t= 9.5 s). This new type of fishbones were designated as hybrid fishbones [6] since they have characteristics of both precessional and diamagnetic fishbones. The hybrid fishbones evolve then to a regime where both types of fishbones (precessional and diamagnetic) are observed simultaneously (around t= 9.75 s). However, when this occurs, both types of fishbones reach only small amplitudes. Gradually the high frequency fishbones disappear and only the low frequency fishbones remain, while its amplitude increases. The regime of diamagnetic fishbones is then reached. Finally, a sawtooth crash occurs and the precessional fishbones regime is restored.

3. Regions of stability

To analyse the fishbones behaviour it is used a qualitative approach based on a variational method. The first step consists in determine the regions of stability for each branch of the internal kink mode in the space of the relevant parameters ($\beta_h, \omega_{*i}, \gamma_I$).The second step will consist in to determine how these parameters evolve during a monster sawtooth and the third to evaluate how this affect fishbones behaviour. The dispersion relation for the internal kink mode including fast ion, resistive and diamagnetic effects in the large aspect ratio circular cross-section approximation is given by [7-9],

$$\delta W_{MHD} + \delta W_{HOT} - \frac{8i\Gamma\left[\left(\Lambda^{3/2}+5\right)/4\right]\left[\omega\left(\omega-\omega_{*i}\right)\right]^{1/2}}{\Lambda^{9/4}\Gamma\left[\left(\Lambda^{3/2}-1\right)/4\right]\omega_A} = 0 \tag{1}$$

where, $\Lambda = -i\left[\omega\left(\omega-\hat{\omega}_{*e}\right)\left(\omega-\omega_{*i}\right)\right]^{1/3}/\gamma_R$, $\gamma_R = S^{-1/3}\omega_A$ is the resistive growth rate, S is the magnetic Reynolds number, ω_A is the Alfven frequency, ω_{*e} is the electron diamagnetic frequency $\omega_{*e} = \left(en_eBr\right)^{-1} dP_e/dr$, P_e and n_e are the electron pressure and density respectively and $\hat{\omega}_{*e} = \omega_{*e} + 0.71\left(eBr\right)^{-1} dT_e/dr$. The Euler gamma functions in equation (1) come from the inertial layer and are evaluated at the q=1 surface. To establish the regions of stability for each branch it is only necessary to determine when the stability of the mode changes, i.e, when the imaginary part of the complex frequency is zero. To proceed, the ideal limit is assumed. Considering an ICRH driven fast ions population characterized by a single normalized magnetic momentum $\lambda \equiv \mu B_0/E = 1$ (on-axis heating) and a Maxwellian distribution in energy, the threshold condition $\mathrm{Im}(\omega) = 0$ is given by,

$$\gamma_I = \frac{3}{4}\left[\frac{\omega}{\langle\omega_D\rangle}\left(\frac{\omega}{\langle\omega_D\rangle} - \frac{\omega_{*i}}{\langle\omega_D\rangle}\right)\right]^{\frac{1}{2}}\left(\frac{\omega}{\langle\omega_D\rangle}\right)^{-\frac{3}{2}}\left[\frac{1}{2} + \frac{\omega}{\langle\omega_D\rangle} + \left(\frac{\omega}{\langle\omega_D\rangle}\right)^{\frac{3}{2}} \mathrm{Re}\, Z\left[\left(\frac{\omega}{\langle\omega_D\rangle}\right)^{\frac{1}{2}}\right]\right], \tag{2}$$

with the corresponding value of β_h given by,

$$\beta_h = \frac{3}{4}\frac{\varepsilon\omega_A}{\pi^{1/2}\langle\omega_D\rangle}\left[\frac{\omega}{\langle\omega_D\rangle}\left(\frac{\omega}{\langle\omega_D\rangle} - \frac{\omega_{*i}}{\langle\omega_D\rangle}\right)\right]^{\frac{1}{2}} e^{\omega/\omega_D}\left(\frac{\omega}{\langle\omega_D\rangle}\right)^{-\frac{5}{2}}. \tag{3}$$

When ω_{*i} and $\langle\omega_D\rangle$ are of the same order of magnitude, β_h is a monotonic function of ω and equation (2) has two solutions provided that $\gamma_I < \gamma_M$, where γ_M is the maximum possible value for the right hand side of equation (2). These two solutions can be drawn in the plan

(β_h, γ_I), where they make approximately a triangle with the line $\gamma_I = 0$. The diamagnetic frequency ω_{*i} plays the role of a parameter determining the location of the top of the triangle.

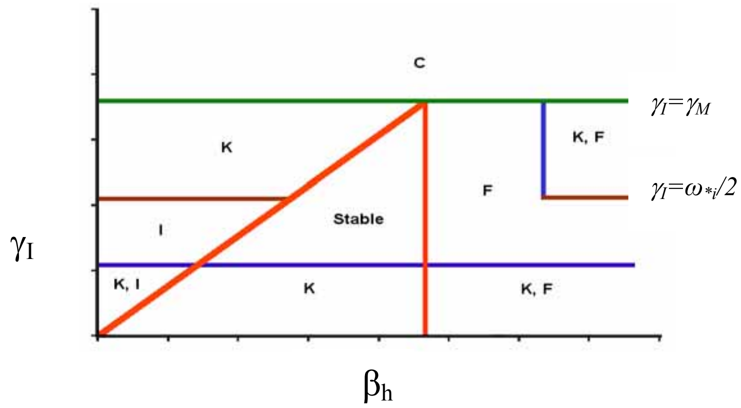

Figure 2: Regions of stability for the different branches in the space of parameters. In the regions labelled with K, I and F, the kink, ion and fishbone branches respectively are unstable. In the region labelled with C, the high and low frequency modes coalesce.

The two solutions of equation (2), represented by red lines in figure 2, correspond to the values of β_h above which the high frequency branch (the fishbone branch) is unstable and below which one of the low frequency branches is unstable. If $\gamma_I > \omega_{*i}/2$ the unstable branch is the kink branch, while if $\gamma_I < \omega_{*i}/2$ the unstable branch is the ion branch. For $\gamma_I > \gamma_M$ the high frequency branch and low frequency branches coalesce and the stable window in β_h vanishes. To complete the diagram, a blue horizontal line was included in order to traduce the resistive effects that were dropped during the calculations and that may turn the kink branch unstable if γ_I is small. The location of this line depends on the magnetic Reynolds number. A blue vertical line was also added in order to traduce finite orbit width effects, which are not included in equation (2). When the fast ions temperature is high enough, the orbits of the fast ions become large and sawtooth stabilisation by fast ions lose its efficiency, so, for high values of β_h sawtooth may become unstable again.

4. Evolution of fishbones behaviour

Having established the regions of stability for each of the branches as function of the relevant parameters (β_h, ω_{*i}, γ_I), the next step consists in evaluate how these parameters evolve during the period of a monster sawtooth. The ideal growth rate γ_I is expected to increase, since γ_I scales with r_1^3 [10], where r_1 is the radius of the q=1 surface, and the q=1 surface expands between sawtooth crashes as consequence of magnetic diffusion. This is confirmed by experimental observations, comparing the inversion radius of monster sawteeth with the inversion radius of the precedent small period sawtooth: The inversion radius is much smaller in the case of the small period sawtooth, which strongly suggests that the q=1 radius has a significant increase during the period of the monster sawtooth. The diamagnetic frequency also increases significantly between sawtooth crashes. $f_{*i} = \omega_{*i}/2\pi$ was previously estimated to be below 3 kHz after sawtooth crashes [5] (regime of short sawteeth). This frequency reaches above 10 kHz when diamagnetic fishbones are first observed and around 20 kHz before the monster crash. These values can be observed directly from the spectrogram since the initial frequency of the diamagnetic fishbones is around f_{*i}. Diagnostics corroborate that ω_{*i}

increases, showing that both the density and temperature profiles of the bulk ions peak during a monster sawtooth. Finally, for β_h, it is assumed that it increases slowly between fishbones bursts and that it decreases abruptly during a fishbone burst as the fast ions are expelled from the plasma centre. This behaviour is well established in fishbones theory [2, 3].

The third step consists now in determine how the evolution of the parameters ($\beta_h, \omega_{*i}, \gamma_I$) affect fishbones behaviour. In the beginning of the monster sawtooth period the plasma is in a state (blue cross in fig. 3) that corresponds to the region of the stability diagram where the fishbone branch is unstable, i.e., with β_h above both solutions of the marginal equation. As a precessional burst is initiated, β_h decreases and the fishbone branch will eventually become stable (see figure 3, left). When this happens, the mode amplitude starts decreasing until the fishbone burst ends. β_h will then increase slowly until a new fishbone burst be triggered.

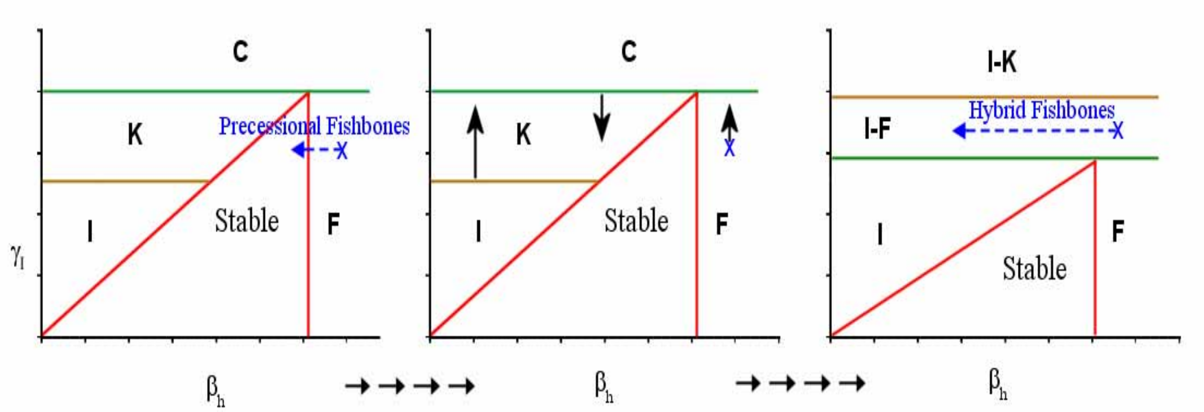

Figure 3: Evolution of the regions of stability during the sawtooth free period.

As γ_I increases, the cross representing the state of the plasma moves upward in the plan (β_h, γ_I), while the increase in ω_{*i} causes the borders of the regions of stability to change: the brown line corresponding to $\gamma_I = \omega_{*i}/2$ moves upward and the green line corresponding to $\gamma_I = \gamma_M(\omega_{*i})$ moves downward (see figure 3, middle). Thus, the increases in γ_I and ω_{*i} will cause the coalescence region to be reached. The unstable branch is now the coalescent ion-fishbone branch, which is unstable for all values of β_h and behaves like the fishbone branch at high β_h and like the ion branch at low β_h (these values depend on ω_{*i}). When a fishbone burst is initiated at high β_h it starts as a "precessional burst", since at high β_h the coalescent ion-fishbone mode behaves like the fishbone mode. However, the decrease in β_h during the burst no longer causes the stable region to be accessed. Instead, the coalescent ion-fishbone mode remains unstable as β_h decreases while its behaviour changes to a "diamagnetic behaviour" and the burst that started as a "precessional" gradually becomes "diamagnetic". This mechanism causes hybrid fishbones to occur. As ω_{*i} continues to increase during the sawtooth free period, the coalescent ion-fishbone mode behaviour becomes "more diamagnetic" and reaches a state where the "precessional behaviour" is no longer dominant over the "diamagnetic behaviour". At this point, small amplitude bursts of both types are triggered independently and can occur simultaneously. Finally, the diamagnetic behaviour becomes dominant and the coalescent mode behaves just like the ion mode producing diamagnetic bursts.

5. Numerical results

The interaction between a mode with an internal kink structure and populations of ICRH driven fast ions was also investigated numerically with the CASTOR-K code [11], which uses the eigenmode calculated by the MISHKA code [12]. A more accurate eigenmode and mode growth rates can be calculated with the NOVA-K code [13]. The CASTOR-K calculates the resonant transference of energy δW_{HOT} between the fast particles population and the mode, which is presented in figure 4 for different values of T_{HOT} as function of the mode frequency.

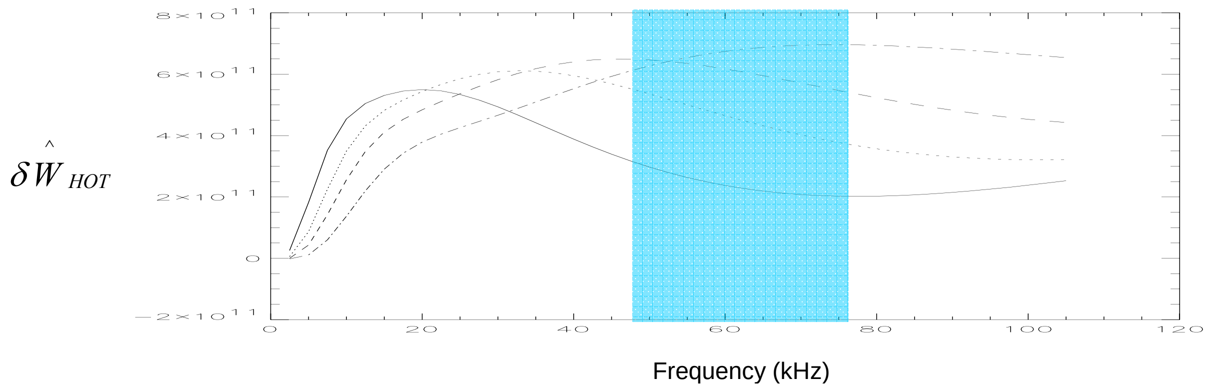

Figure 4: Resonant transference of energy between the internal kink mode and an ICRH driven fast ions population with temperatures of 500 keV (solid line), 750 keV (dotted), 1 MeV (dashed) and 1.5 MeV (dashed/dotted). The observed frequency of precessional fishbones is shadowed.

Figure 4 shows that the best fit between experimental and numerical results is for a fast ions temperature T_{HOT} between 1 MeV and 1.5 MeV, while the value of T_{HOT} estimated for these experiments was around 1 MeV. It can also be seen that the mode expected frequency increases rapidly as the fast ions temperature increases.

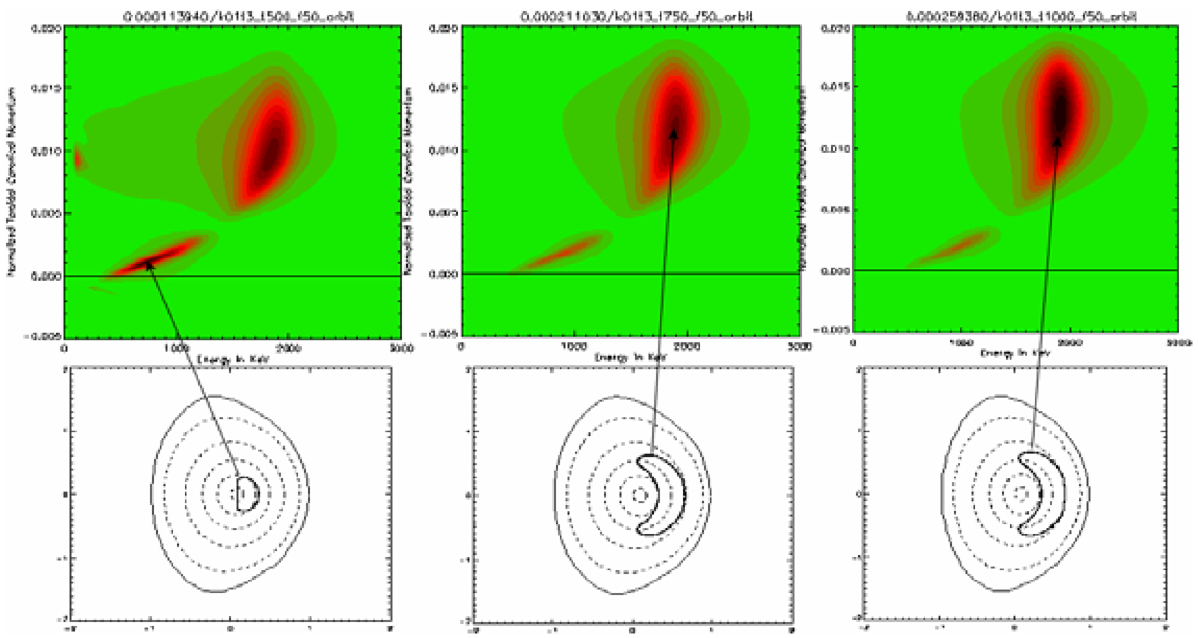

Figure 5: Upper line - Resonant transference of energy between the internal kink mode (f=50 kHz) and an ICRH driven fast ions population as function of the energy and the toroidal canonical moment for three different fast ions temperatures: 500 keV (left), 750 keV (middle) and 1000 keV (right). Lower line: Orbits of the particles with a stronger interaction with the node, for each case.

Figure 5 (upper half) shows the resonant transference of energy between the internal kink mode (f=50 kHz) and three ICRH driven fast ion populations characterized by different temperatures (500, 750 and 1000 keV). The orbits of the particles in stronger resonance with the mode are also represented in figure 5 (lower half). It can be seen that there are two main resonances, one corresponding to particles nearer the magnetic axis centred around 900 keV and the other corresponding to particles farer from the plasma axis centred around 1.8 MeV. This second resonance becomes dominant when the fast ions temperature increases (it is already dominant for T_{HOT}=750 keV). The change in the type of orbits of the particles strongly interacting with the mode may contribute to explain the high frequency of the precessional fishbones observed experimentally.

6. Summary and conclusions

In JET experiments with low density plasmas, when sawtooth are stable, the absence of crashes allows the bulk ions pressure profile to peak. This causes a significant increase in the diamagnetic frequency and under these circumstances the high frequency branch solution of the internal kink dispersion relation coalesces with the low frequency branch. The coalescent ion-fishbone mode is always unstable and behaves like the ion mode for low values of β_h and like the fishbone mode for high values of β_h. Two new fishbone regimes were observed: a regime of hybrid fishbones is observed when the ion-fishbone mode is unstable with dominant precessional behaviour and a regime where small amplitude precessional and diamagnetic bursts occur simultaneously is observed when the ion-fishbone mode is unstable but none of the behaviours is dominant. It was also found that the particles in resonance with the internal kink high frequency branch can have two types of orbits. The main resonance in the space (E, P_φ) changes when increasing the fast ions temperature, which may cause a considerable increase in the mode frequency.

Aknowledgments

This work, supported by the European Communities and “Instituto Superior Técnico” under the Contract of Association between EURATOM and IST, has been carried out within the framework of the European Fusion Development Agreement. Financial support was also received from “Fundação para a Ciência e Tecnologia” in the frame of the Contract of Associated Laboratory. The views and opinions expressed herein do not necessarily reflect those of the European Commission, IST and FCT.

References

[1] – K. McGuire *et al*. Phys. Rev. Lett. **50** 891 (1983)
[2] – L. Chen, R. White and M. Rosenbluth, Phys. Rev. Lett. **52** 1122 (1984)
[3] – B. Coppi and F. Porcelli, Phys. Rev. Lett. **57**, 2272 (1986)
[4] – M. Bussac *et al*. Phys. Rev. Lett. **35**, 1638 (1975)
[5] – M. Mantsinen *et al*. Plasma Phys. Control. Fusion **42**, 1291, (2000)
[6] – F. Nabais *et al*. Phys. Plasmas 12, 102509 (2005)
[7] – R. White, L.Chen, F. Romanelli and R. Hay, Phys. Fluids **28**, 278 (1985)
[8] – R. White, M. Bussac and F. Romanelli, Phys. Rev. Lett. **62**, 539 (1989)
[9] – R. White, F. Romanelli and M. Bussac, Phys. Fluids B **2**, 745 (1990)
[10] – C. K. Phillips *et al*. Phys. Fluids B **4** (7), 2155 (1995)
[11] – D. Borba and W. Kerner, J. Computational Physics **153**, 101 (1999)
[12] – A. B. Mikhailovskii *et al*. Plasma Physics Reports **10**, 844 (1997)
[13] – N. N. Gorelenkov, C. Cheng, V. Kiptily, M. Mantsinen and S. E. Sharapov, Proc. 20th IAEA Fusion Energy Conference 2004, (Vilamoura, 2004) (Vienna: IAEA), paper TH/5-2 Rb